



Effect of Cu content on microstructure, morphology, and antibacterial properties of Ti-Cu alloy thin films

Chittra KEDKAEW¹, Phalakorn KHWANSUNGNOEN², and Tanattha RATTANA^{3,*}

¹ Department of Physics, Faculty of Science, King Mongkut's University of Technology Thonburi, Bangkok, 10140, Thailand

² Nuclear Technology Research and Development Center, Thailand Institute of Nuclear Technology (Public Organization), Nakhon Nayok, 26120, Thailand

³ Department of Physics, Faculty of Science, Burapha University, Chonburi, 20131, Thailand

*Corresponding author e-mail: tanattha@go.buu.ac.th

Received date:

26 February 2025

Revised date:

29 April 2025

Accepted date:

11 December 2025

Keywords:

Ti-Cu alloy;
Thin film;
Co-sputtering;
Microstructure;
Antibacterial properties

Abstract

Ti-Cu alloy thin films exhibit considerable potential for the development of advanced antibacterial surfaces, particularly for biomedical applications. In this research, Ti-Cu binary alloy thin films with a wide range of Cu content from 25.8 at% to 77.8 at% were deposited using magnetron co-sputtering with pure Ti and Cu as the targets. The composition of Cu in the films can be controlled by the applied power of Cu targets. This study investigated the effect of Cu content on the microstructural, morphological, and antibacterial properties using X-ray diffraction (XRD), Field emission scanning electron microscopy (FESEM), Atomic force microscopy (AFM), X-ray photoelectron spectroscopy (XPS) and plate-count method, respectively. Structural analysis using XRD revealed that Ti (Cu) solid solution is formed for the Ti-Cu coatings with the Cu contents of 25.8 at% and the films tended to form an amorphous structure embedded with Cu nanocrystals when the Cu content was 77.8 at%. Surface morphology showed that the films with higher Cu content exhibited increased surface roughness and the presence of Cu nanogranular features. Antibacterial evaluations against *Escherichia coli* showed that the films containing Cu in the range of 25.8 at% to 77.8 at%. This effect is attributed to both inherent antibacterial properties by Cu and the microstructural modifications that enhance bacterial inhibition.

1. Introduction

Titanium (Ti) has several intriguing properties, such as lightweight, a high melting point, and excellent biocompatibility, making it suitable for use in medical materials. Additionally, its high oxidation resistance and strength enable Ti can be used in various applications, including engine components and the automotive industry [1-3]. The addition of other metals can significantly enhance the properties of Ti. One well-known example is the Ti-Ni alloy, commonly referred to as Nitinol. This alloy is extensively studied in the medical field due to its unique characteristics, such as super elasticity and the shape memory [4-6]. Alloying Ti with niobium (Nb) can reduce its elastic modulus. This reduction helps to minimize stress shielding, which is a common problem in implant materials. Ti-Nb alloys are particularly promising for orthopedic applications due to their excellent biocompatibility, low cytotoxicity, and high corrosion resistance [7,8]. Another notable alloy is Ti-Zr alloy, which has gained attention for its excellent biocompatibility and mechanical properties. The addition of zirconium (Zr) to Ti improves its strength, corrosion resistance, and wear resistance, making it highly suitable for biomedical applications, particularly in dental and orthopedic implants [9,10].

Copper (Cu) is another element widely used to improve the properties of Ti alloys. Due to its good electrical and thermal conductivity,

as well as its widely recognized antibacterial properties. Therefore, combining these metals in the form of a Ti-Cu thin film integrates their advantageous features, resulting in a multifunctional material that offers both mechanical strength and antibacterial benefits. This makes Ti-Cu alloys highly promising for medical applications [11-13]. ChangBo *et al.* [14] prepared Ti-Cu alloys by Ar-arc melting followed by heat treatment and they showed that Ti alloyed with a small amount of Cu (1 wt% to 5 wt%) exhibits suitable mechanical properties, good biocompatibility, and excellent corrosion resistance. Additionally, Ti alloys containing at least 5 wt% Cu displayed a good antibacterial rate (over 99%) against *E. coli* and *S. aureus*. Stranak *et al.* [15] demonstrated that Ti-Cu films produced via high power impulse magnetron sputtering can efficiently kill bacteria over 1 day to 10 day. The antibacterial mechanism of Ti-Cu alloys was multifaceted, involving both the released Cu ions disrupting cellular processes and physical effects from direct contact with the alloy surface [16,17]. Moreover, The antibacterial capability of Ti-Cu alloys is also related to the formation of the Ti₂Cu phase, finer Ti₂Cu phases potentially resulted in improved antibacterial performance [18].

In recent years, Ti-Cu alloys have been successfully fabricated in the form of thin films. Ti-Cu alloy thin film fabrication approach offers several advantages, particularly for the development of antibacterial surfaces [13,15,19]. Magnetron sputtering is frequently used

to make thin films of Ti-Cu alloy. This method is preferred for its ability to produce thin films with high density, excellent surface uniformity, and strong adhesion to the substrate. Magnetron sputtering can be performed using various types of targets, such as a single alloy target or through co-sputtering from multiple targets. The single alloy target method offers many advantages such as improved uniformity of the thin film and operational simplicity, the composition of the deposited film closely matches with the target material [20]. However, this method has limitations in compositional flexibility due to the fixed alloy content of the target. As a result, creating a new target for each desired film composition can be both costly and time-consuming. In contrast, co-sputtering involves simultaneously sputtering from different targets. This method provides significant flexibility in adjusting alloy composition by independently controlling the amount of each element from the targets through varying the power applied to each target [21].

In this research, Ti-Cu alloy thin films were deposited on substrates using the magnetron co-sputtering technique with pure Ti and Cu as the targets. The Cu content in the films was controlled by varying the power applied to the Cu target. The effect of Cu content on the microstructure, surface morphology, and antibacterial performance of the Ti-Cu films was investigated.

2. Experimental

2.1 Thin film preparation

The Ti-Cu alloy thin films were deposited onto silicon wafers and aluminum substrates using a DC magnetron co-sputtering system, with Ti (99.99%) and Cu (99.97%) as targets. Prior to deposition, the chamber was evacuated to a base pressure of 5.0×10^{-5} mbar using a diffusion pump backed by a rotary vane pump. Ultra-high purity argon (99.999%) was introduced into the chamber at a constant flow rate of 4.0 sccm to maintain a working pressure of 5.0×10^{-3} mbar. The Ti and Cu targets were pre-sputtered for 5 min to eliminate surface contamination. The deposition duration was consistently set at 10 min for all films. The composition of the Ti-Cu alloy thin films was varied by adjusting the Cu magnetron sputtering power within the range of 12 W to 162 W, while the Ti target was sputtered at a constant power of 250 W for all conditions. The parameters used for the deposition of the Ti-Cu thin films were summarized in Table 1.

2.2 Thin film characterization

A grazing incidence X-ray diffractometer (GIXRD, Rigaku SmartLab) with a Cu K α X-ray source (1.54 Å) was used to analyze the crystalline structure of Ti-Cu alloy thin films at an incident angle of 1.0 degrees. The cross-sectional and surface morphology of the thin films was visualized using a Field emission scanning electron microscope (FESEM, Hitachi SU-8030). The elemental composition of the thin films was determined through Energy-dispersive x-ray spectroscopy (EDX). The surface roughness of the thin films was measured with an Atomic force microscope (AFM, Hitachi Hi-Tech SPA400). The chemical states of the obtained films were assessed using an X-ray photoelectron spectrometer (XPS, Kratos AXIS Ultra DLD). The antibacterial activity of the Ti-Cu thin film against *Escherichia coli*

(*E. coli*) was tested using the plate count method (JIS Z2801:2000 standard) and compared to an aluminum plate. Samples were incubated at 37°C with a bacterial suspension of 105 CFU·mL⁻¹ to 106 CFU·mL⁻¹ for 24 h. After incubation, the samples were serially diluted with PBS 101, 102, 103, 104, and 105-fold and 100 μ L of each dilution was plated onto Muller-Hinton Agar (MHA) for 24 h at 37°C. The viable bacteria were quantified by counting the colonies on the MHA plates.

3. Results and discussion

The elemental composition of the sputtered Ti-Cu alloy thin films was presented in Table 2. The results demonstrated that the Cu content increased with heightened power levels applied to the Cu target. In particular, the Cu content in the thin films was 25.8 at%, 44.5 at%, 64.5 at%, and 77.8 at% at the power settings of 12 W, 27 W, 93 W, and 162 W for the Cu target, respectively. Notably, even though the power applied to the Cu target (93 W) was lower than the power applied to the Ti target (250 W), the Cu content in the film exceeded that of the Ti content. This phenomenon was explained by the fact that Cu has a higher sputtering yield (~2.3) than Ti (~0.6).

Table 1. Deposition parameter of Ti-Cu alloy thin films.

Parameters	Details
Sputtering target	Ti, Cu
Substrate	Si wafer
Target-substrate distance	13 cm
Base pressure	5.0×10^{-5} mbar
Total pressure	5.0×10^{-3} mbar
Argon flow rate	4.0 sccm
Ti Target Power	250 W
Cu Target Power	12 W to 162 W
Deposition time	10 min

Table 2. The EDX composition of Ti-Cu thin films with deposited at different powers of Cu target.

Sample	Target power [W]		EDX [atomic%]	
	Ti	Cu	Ti	Cu
1	250	12	74.2	25.8
2	250	27	55.5	44.5
3	250	93	35.5	64.5
4	250	162	22.2	77.8

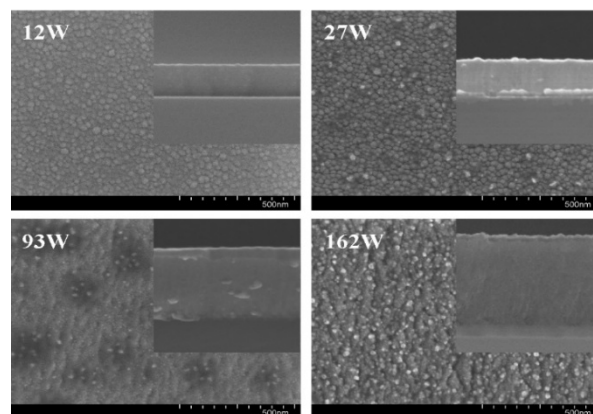


Figure 1. FESEM images of Ti-Cu alloy thin films at different powers of Cu target.

Figure 1 showed the surface morphologies and cross-sectional FESEM images of Ti-Cu thin films deposited at different Cu target power. The results indicated that the surface morphology of the coatings was greatly impacted by increasing the Cu target power. The Cu content increased in the film as a function of Cu target powers. At a Cu target power of 12 W, the film surface was uniform with evenly distributed nanoscale grains that showed a Cu content of 25.8%. As the Cu target power was increased to 27 W, it resulted in a composition of 44.5 at% Cu with increasing grain size. When the Cu content reached 64.5 at% at a Cu target power of 162 W, the film surface appeared denser and smoother, suggesting an amorphous structure. At 77.8 at% Cu, nano-granular Cu was dispersed throughout the film surface. The average thickness of the Ti-Cu alloy thin films was 100 nm, 140 nm, 190 nm, and 250 nm for films deposited at Cu target powers of 12 W, 27 W, 93 W, and 162 W, respectively. The increase in thickness was due to the higher deposition rate when increasing the input power to the Cu target.

Figure 2 showed the 3D AFM images of Ti-Cu alloy thin films prepared by varying Cu target powers ranging from 12 W to 162 W. Table 3 summarized the root mean square (RMS) roughness of the thin films. According to the AFM images, all thin films exhibited smooth and crack-free surfaces. The roughness increased as the Cu target power rose. This event was attributed to the effects of higher sputtering power, which could increase the kinetic energy and surface mobility of adatoms that arrived at the substrate. Enhanced mobility of these adatoms was essential for the formation of continuous films and encouraged the development of larger grains and other morphological features. Additionally, the increase in sputtering power improves the surface diffusion of these adatoms by providing additional momentum transfer to the expanding surface.

Figure 3 presents the GIXRD patterns of Ti-Cu alloy thin films deposited at different Cu target powers. For the thin film deposited at 12 W Cu target power, a prominent peak was observed at approximately 38°, corresponding to the (002) plane of hexagonal close-packed (hcp) Ti (JCPDS no. 44-1294). When the Cu target power was increased to 27 W, the XRD patterns remained similar, with no detectable Cu phase, indicating the formation of a solid solution of Cu and Ti within the hcp structure. A broad XRD peak between 35° and 47° at a 93 W Cu target indicated lattice distortions brought on by variations in atomic size, which reduce the crystallinity of the film. Demonstrating that the thin film was predominantly amorphous. It agreed with the characteristics of amorphous metallic alloys containing a high content of Cu [22,23]. At a Cu target power of 162 W, the amorphous structure persisted, but a new peak emerged at approximately 49°, corresponding to the (200) plane of crystalline Cu (JCPDS Card No. 85-1326). At higher Cu concentrations, it appeared that nanocrystalline Cu formed within the thin film. This phenomenon occurred because the mobility of adatoms on the surface improved with increasing power applied to the Cu target. The higher energy of the adatoms led to the formation of larger Cu crystallites. As a result, this process produced highly crystalline Cu films. The absence of intermetallic phases such as Ti_2Cu or Ti_3Cu in the deposited Ti-Cu alloy thin film was attributed to the low-energy nature of the deposition process, particularly in the absence of external heating or thermal treatment [24,25]. Under these conditions, the adatoms deposited on the substrate lack sufficient

mobility and energy to diffuse and rearrange into the long-range ordered structures required for intermetallic phase formation.

The diffraction peak of the thin films was fitted using a Gaussian function to extract the peak position (2θ) and Full width at half maximum (FWHM). These parameters were subsequently used to estimate the average crystallite size via the Scherrer equation. The variations in 2θ , FWHM, and crystallite size as a function of the applied Cu target power are shown in Figure 4. With increasing input power to the Cu target, the diffraction peak position shifts toward higher 2θ values, indicating a reduction in the average interatomic spacing within the amorphous phase. This behavior can be explained by the difference in atomic radii between Ti ($\approx 1.47 \text{ \AA}$) and Cu ($\approx 1.28 \text{ \AA}$). The replacement of larger Ti atoms with smaller Cu atoms results in a more compact atomic packing, thereby decreasing the average interatomic distance.

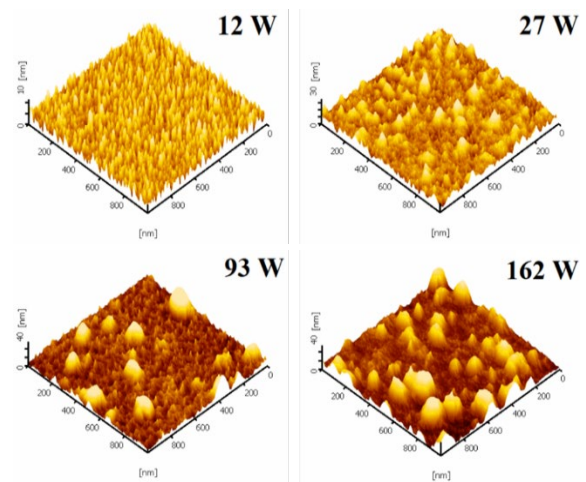


Figure 2. AFM images of Ti-Cu alloy thin films at different powers of Cu target.

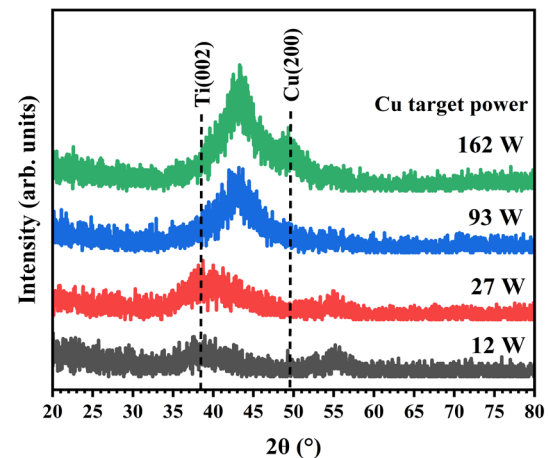


Figure 3. GIXRD patterns of the Ti-Cu thin films at different powers of the Cu target.

Table 3. RMS roughness of Ti-Cu thin films at different powers of Cu target.

Cu target power [W]	RMS roughness [nm]
12	1.5
27	3.7
93	7.5
162	9.1

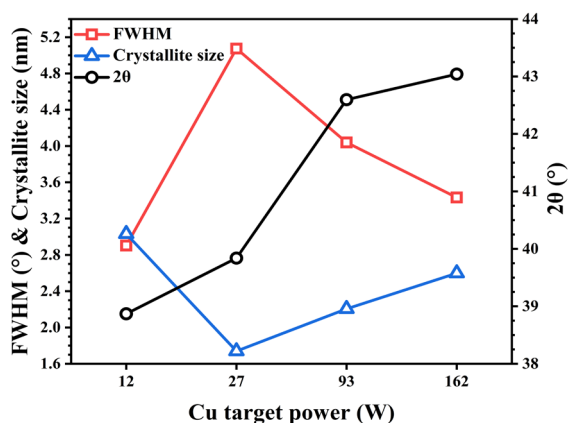


Figure 4. Peak position, FWHM and crystallite size value of of the Ti-Cu thin films at different powers of the Cu target.

Consistently, the FWHM exhibits a pronounced increase at a Cu target power of 27 W, accompanied by a reduction in the calculated crystallite size, which can be ascribed to the structural transition from crystalline Ti to an amorphous configuration. The incorporation of Cu atoms disrupts the long-range order of the Ti lattice and promotes the formation of a glassy phase. When the Cu target power was increased to 93 W and 162 W, the FWHM decreased and the calculated crystallite size became larger. This behavior may be related to the effect of Cu addition, which promotes short-range order and the formation of nanoscale atomic clusters, leading to a narrowing of the diffraction peak and an increase in the apparent crystallite size, even though the films largely retain their amorphous character.

Film structure and properties of Ti-Cu metallic glass thin films are strongly influenced by sputtering power. Higher Cu target power increases Cu content and film thickness induces nanoscale Cu clustering and slight local ordering and raises the proportion of metallic Cu. Grain size, surface density, and roughness are also enhanced, promoting morphological evolution.

The chemical state of Ti-Cu alloy thin films deposited at different Cu target powers was analyzed using XPS, as shown in Figure 5. High-resolution XPS spectra of the Cu 2p signals and the relative curve-fitting analysis for the thin films deposited at Cu target powers of 12 W and 162 W were shown in Figure 5(a-b). Three peaks were observed in the Cu 2p_{3/2} region at 932.6 ± 0.1 eV, 933.6 ± 0.2 eV, and 934.8 ± 0.1 eV. Metallic Cu (Cu(0)) was represented by the first peak (932.6 ± 0.1 eV) [26,27]. CuO was represented at the second peak (933.6 ± 0.2 eV), while Cu(II) in the hydroxide state was associated with the third peak (934.8 ± 0.1 eV). The formation of CuO in the Ti-Cu thin films was primarily attributed to the oxidation of Cu upon exposure to ambient air. In contrast, the Cu(II) hydroxide phase was considered a metastable phase that may convert into the more thermodynamically stable CuO under ambient or aqueous conditions [28]. The detection of the Cu(II) hydroxide phase on the film surface indicated that it likely formed as a result of Cu's inherent reactivity, specifically through oxidation and hydration processes upon exposure to environmental oxygen and moisture. According to the results, the intensity of Cu(0) increases with increasing Cu target power because the enhanced Cu deposition rate and promotes metallic bonding and cluster formation at the thin film surface, which further contributes to the higher intensity of Cu(0) observed in the XPS spectra.

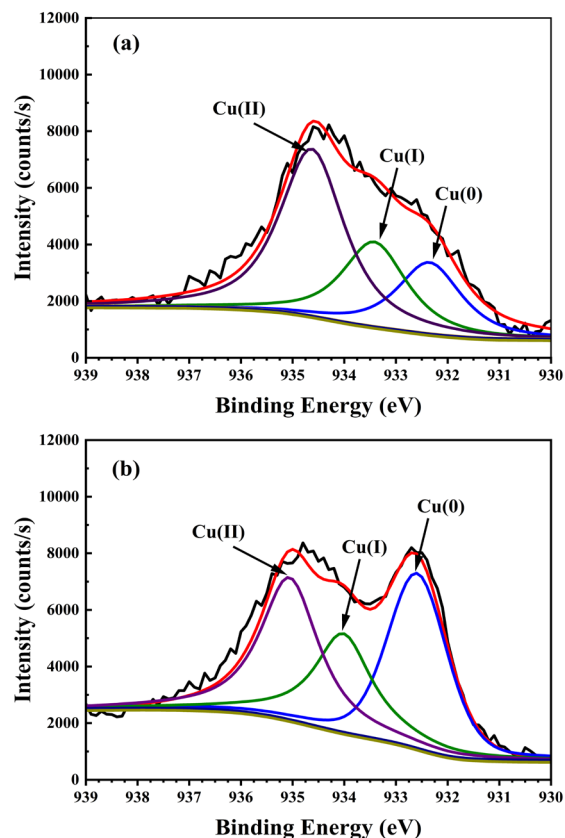


Figure 5. High resolution XPS spectra of Cu 2p signals of Ti-Cu alloy thin films at Cu target power (a) 12 W, and (b) 162 W.

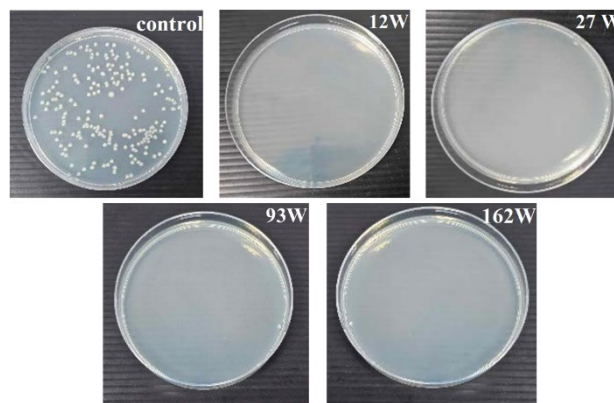


Figure 6. Photos of colony forming units of *Escherichia coli* after contact with control and Ti-Cu alloy thin films for 24 h.

Figure 6 illustrated the colonization of *E. coli* on the Ti-Cu alloy thin film after 24 h of incubation. The control sample (aluminum plate) displayed numerous *E. coli* colonies, while the Ti-Cu sample showed no colonies at all, indicating the powerful antibacterial activity of the Ti-Cu thin film against *E. coli*. The addition of Cu to alloy thin films significantly enhanced antibacterial properties through various interacting mechanisms. One primary mechanism involved the release of Cu ions when bacteria contacted a surface of sample containing the Cu. These Cu ions are released from the surface of a thin film and moved to the bacterial cell wall via electrostatic forces. This interaction limited bacterial activity, interfered with metabolic processes, and led to bacterial cell death [16]. The prepared Ti-Cu alloy thin films

often exhibited nanocrystalline Cu or Cu nanoparticles, which provided a high surface-area-to-volume ratio. The increase in surface area could enhance the release of Cu ions, especially in moist environments or upon contact with bacterial cells [29]. Moreover, Cu can induce the generation of reactive oxygen species (ROS), including superoxide anions (O_2^-), hydrogen peroxide (H_2O_2), and hydroxyl radicals ($^{\bullet}OH$), primarily via redox reactions such as Haber-Weiss reactions. These ROS possess strong oxidative properties and can cause severe bacterial damage. An increase in metallic copper (Cu(0)) in Ti-Cu thin films significantly influences both the ion release behavior and antibacterial efficiency. XPS analysis confirms the presence and valence states of copper near the surface, which are critical for antibacterial mechanisms. Embedded Cu(0), often located beneath the surface, acts as a stable reservoir that continuously replenishes surface Cu ions consumed during antibacterial reactions, ensuring long-term efficacy. Surface-exposed Cu(0) promotes rapid and concentrated release of Cu ions through oxidation to Cu(I) and Cu(II), facilitating reactive oxygen species (ROS) generation and immediate bacterial inactivation. High Cu(0) content also supports the formation of highly active phases, such as $Cu(OH)_2$ and Cu_2O , essential for ROS-mediated contact killing. Additionally, the nano roughness of the prepared film increased the effective surface area and enhanced physical contact between bacteria and the film. This intimate interaction exposes bacterial cells to more Cu-containing regions and strengthens the local ion-exchange interface. As a result, the rough surface promotes a higher local concentration of released Cu ions at the bacteria-surface interface, thereby intensifying membrane disruption and improving antibacterial efficiency [13,16,30].

4. Conclusions

Ti-Cu alloy thin film with Cu content in the range of 25.8 at% to 77.8 at% were successfully prepared by DC magnetron co-sputtering. This process involved varying the power applied to the Cu target from 12 W to 163 W. The Cu content in the alloy thin films had a significant impact on their crystal structure, morphology, and antibacterial properties. Adding Cu generally increased the surface roughness of the thin films. Antibacterial tests demonstrated that Ti-Cu alloy thin films containing more than 25.8 at% of Cu exhibited good antibacterial properties and are effective in killing *E. coli* bacteria. These results suggested that the incorporation of Cu not only modifies the microstructure and surface characteristics but also plays a critical role in improving the antibacterial performance of thin films, making them promising candidates for biomedical surface coatings.

Acknowledgements

This work was financially supported by (i) Burapha University (BUU), (ii) Thailand Science Research and Innovation (TSRI), and (iii) National Science Research and Innovation Fund (NSRF). (Fundamental Fund : Grant no. 38/2566)

References

- [1] X. Liu, S. Chen, J. K. Tsoi, and J. P. Matinlinna, "Binary titanium alloys as dental implant materials—a review," *Regenerative Biomaterials*, vol. 4, no. 5, pp. 315–323, 2017.
- [2] P. A. Dearnley, K. L. Dahm, and H. Çimenoglu, "The corrosion-wear behavior of thermally oxidised CP-Ti and Ti-6Al-4V," *Wear*, vol. 256, no. 5, pp. 469–479, 2004.
- [3] M. Geetha, A. K. Singh, R. Asokamani, and A. K. Gogia, "Ti based biomaterials, the ultimate choice for orthopaedic implants—A review," *Progress in Materials Science*, vol. 54, no. 3, pp. 397–425, 2009.
- [4] H. Kahn, M. A. Huff, and A. H. Heuer, "The TiNi shape-memory alloy and its applications for MEMS," *Journal of Micromechanics and Microengineering*, vol. 8, no. 3, p. 213–221, 1998.
- [5] Y. Tong, A. Shuitcev, and Y. Zheng, "Recent development of TiNi-based shape memory alloys with high cycle stability and high transformation temperature," *Advanced Engineering Materials*, vol. 22, no. 4, p. 1900496, 2020.
- [6] R. Karelin, V. Komarov, V. Cherkasov, I. Khmelevskaya, V. Andreev, V. Yusupov, and S. Prokoshkin, "Structure and properties of TiNi shape memory alloy after quasi-continuous equal-channel angular pressing in various aged states," *Metals*, vol. 13, no. 11, p. 1829, 2023.
- [7] M. Marczewski, K. Wiczerzak, X. Maeder, L. Lapeyre, C. Hain, M. Jurczyk, and T. Nelis, "Microstructure and mechanical properties of Ti-Nb alloys: comparing conventional powder metallurgy, mechanical alloying, and high power impulse magnetron sputtering processes for supporting materials screening," *Journal of Materials Science*, vol. 59, no. 20, pp. 9107–9125, 2024.
- [8] E. M. Karakurt, Y. Huang, Y. Cetin, A. Incesu, H. Demirtas, M. Kaya, Y. Yildizhan, M. Tosun, and G. Akbas, "Assessing microstructural, biomechanical, and biocompatible properties of TiNb alloys for potential use as load-bearing implants," *Journal of Functional Biomaterials*, vol. 15, no. 9, p. 253, 2024.
- [9] H. M. Grandin, S. Berner, and M. Dard, "A review of titanium zirconium (TiZr) alloys for use in endosseous dental implant," *Materials*, vol. 5, no. 8, pp. 1348–1360, 2012.
- [10] P. Ji, S. Liu, C. Shi, K. Xu, Z. Wang, B. Chen, B. Li, Y. Yang, and R. Liu, "Synergistic effect of Zr addition and grain refinement on corrosion resistance and pitting corrosion behavior of single α -phase Ti-Zr-based alloys," *Journal of Alloys and Compounds*, vol. 896, p. 163013, 2022.
- [11] S. Rashid, M. Sebastiani, M. Z. Mughal, R. Daniel, and E. Bemporad, "Influence of the silver content on mechanical properties of Ti-Cu-Ag thin films," *Nanomaterials*, vol. 11, no. 2, p. 435, 2021.
- [12] C. Apblett, D. Muira, M. Sullivan, and P. J. Ficalora, "Reaction of Cu-Ti bilayer films in vacuum and hydrogen," *Journal of Applied Physics*, vol. 71, no. 10, pp. 4925–4932, 1992.
- [13] D. Wojcieszak, D. Kaczmarek, A. Antosiak, M. Mazur, Z. Rybak, A. Rusak, M. Osekowska, A. Poniedzialek, A. Gamian, and B. Szponar, "Influence of Cu-Ti thin film surface properties on antimicrobial activity and viability of living cells" *Materials Science and Engineering: C*, vol. 56, pp. 48–56, 2015.
- [14] C. Yi, Z. Ke, L. Zhang, J. Tan, Y. Jiang, and Z. He, "Antibacterial Ti-Cu alloy with enhanced mechanical properties as implant applications," *Materials Research Express*, vol. 7, no. 10, p. 105404, 2020.

- [15] V. Stranak, H. Wulff, H. Rebl, C. Zietz, K. Arndt, R. Bogdanowicz, B. Nebe, R. Bader, A. Podbielski, Z. Hubicka, and R. Hippler, "Deposition of thin titanium–copper films with antimicrobial effect by advanced magnetron sputtering methods," *Materials Science and Engineering: C*, vol. 31, no. 7, pp. 1512-1519, 2011.
- [16] P. Mahmoudi, M. R. Akbarpour, H. B. Lakeh, F. Jing, M. R. Hadidi, and B. Akhavan, "Antibacterial Ti–Cu implants: A critical review on mechanisms of action," *Materials Today Bio*, vol. 17, p. 100447, 2022.
- [17] W. Zhang, S. Zhang, H. Liu, L. Ren, Q. Wang, and Y. Zhang, "Effects of surface roughening on antibacterial and osteogenic properties of Ti–Cu alloys with different Cu contents," *Journal of Materials Science & Technology*, vol. 88, pp. 158-167, 2021.
- [18] E. Zhang, X. Wang, M. Chen, and B. Hou, "Effect of the existing form of Cu element on the mechanical properties, bio-corrosion and antibacterial properties of Ti–Cu alloys for biomedical application," *Materials Science and Engineering: C*, vol. 69, pp. 1210-1221, 2016.
- [19] S. Mahmoudi-Qashqay, M. R. Zamani-Meymian, and S. J. Sadati, "Improving antibacterial ability of Ti–Cu thin films with co-sputtering method," *Scientific Reports*, vol. 13, no. 1, p. 16593, 2023.
- [20] N. Witit-anun, and A. Buranawong, "High-temperature oxidation resistance of CrAlN thin films prepared by DC reactive magnetron sputtering," *Journal of Metals, Materials and Minerals*, vol. 33, no. 3, p. 1600, 2023.
- [21] K. Leelaruedee, K. Taweessup, and P. Visuttipitukul, "Formation of nano-crystalline chromium-zirconium nitride (Cr–Zr–N) film coating by DC unbalanced magnetron sputtering," *Journal of Metals, Materials and Minerals*, vol. 31, no. 4, pp. 69–75, 2021.
- [22] R. L. Zong, S. P. Wen, F. Zeng, Y. Gao, and F. Pan, "Nano-indentation studies of Cu–W alloy films prepared by magnetron sputtering," *Journal of Alloys and Compounds*, vol. 464, no. 1-2, pp. 544–549, 2008.
- [23] M. Ghidelli, A. Orekhov, A. Li Bassi, G. Terraneo, P. Djemia, G. Abadias, M. Nord, A. Béché, N. Gauquelin, J. Verbeeck, J. P. Raskin, D. Schryvers, T. Pardoën, and H. Idrissi, "Novel class of nanostructured metallic glass films with superior and tunable mechanical properties," *Acta Materialia*, vol. 213, p. 116955, 2021.
- [24] A. Ishida, M. Sato, and Z. Y. Gao, "Effects of Ti content on microstructure and shape memory behavior of $Ti_xNi_{(84.5-x)}Cu_{15.5}$ ($x=44.6-55.4$) thin films," *Acta materialia*, vol. 69, pp. 292-300, 2014.
- [25] L. Qin, D. Ma, Y. Li, P. Jing, B. Huang, F. Jing, D. Xie, Y. Leng, B. Akhavan, and N. Huang, "Ti–Cu coatings deposited by a combination of HiPIMS and DC magnetron sputtering: The role of vacuum annealing on Cu diffusion, microstructure, and corrosion resistance," *Coatings*, vol. 10, no. 11, p. 1064, 2020.
- [26] M. C. Biesinger, "Advanced analysis of copper X-ray photoelectron spectra," *Surface and Interface Analysis*, vol.49, no.13, pp. 1325-1334, 2017.
- [27] A. Roy, A. K. Mukhopadhyay, S. C. Das, G. Bhattacharjee, A. Majumdar, and R. Hippler, "Surface stoichiometry and optical properties of $Cu_x-Ti_yC_z$ thin films deposited by magnetron sputtering," *Coatings*, vol. 9, no. 9, p. 551, 2019.
- [28] Y. Cudennec, and A. Lecerf, "The transformation of $Cu(OH)_2$ into CuO , revisited," *Solid State Sciences*, vol. 5, no. 11–12, pp. 1471–1474, 2003.
- [29] I. Salah, E. Allan, S. P. Nair, and I. P. Parkin, "Antibacterial performance of a copper nanoparticle thin film," *Nano Select*, vol. 5, no. 9, p. 2300134, 2024.
- [30] J. Hasan, R. J. Crawford, and E. P. Ivanova, "Antibacterial surfaces: The quest for a new generation of biomaterials," *Trends in Biotechnology*, vol. 31, no. 5, pp. 295–304, 2013.